Applied Physics Letters

RESEARCH ARTICLE | AUGUST 21 2024

Air-coupled ultrasound using broadband shock waves from piezoelectric spark igniters

K. G. Scheuer ; R. G. DeCorby

Appl. Phys. Lett. 125, 082202 (2024)
https://doi.org/10.1063/5.0207969

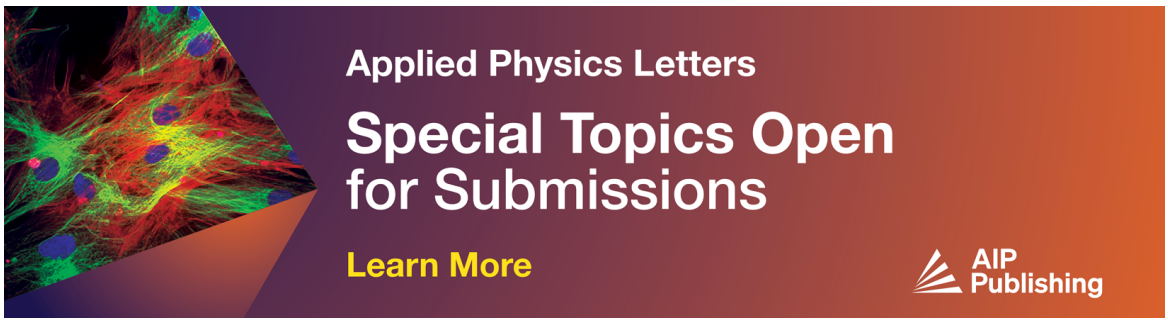

Applied Physics Letters ARTICLE pubs.aip.org/aip/apl

Air-coupled ultrasound using broadband shock waves from piezoelectric spark igniters

Cite as: Appl. Phys. Lett. **125**, 082202 (2024); doi: 10.1063/5.0207969
Submitted: 12 March 2024 · Accepted: 11 August 2024 ·
Published Online: 21 August 2024

K. G. Scheuer[1,2] and R. G. DeCorby[2,a)]

AFFILIATIONS

[1]Ultracoustics Technologies Ltd., Sherwood Park, Alberta T8A 3H5, Canada
[2]ECE Department, University of Alberta, 9211-116 St. NW, Edmonton, Alberta T6G 1H9, Canada

[a)]Author to whom correspondence should be addressed: rdecorby@ualberta.ca

ABSTRACT

We used an optomechanical sensor to study the ultrasound generated by manually operated piezoelectric spark igniters. These low-energy sparks produce short-duration acoustic shock-wave pulses, with sub-microsecond rise times and frequency content extending well beyond 2 MHz in air. The same source–receiver combination was then used to demonstrate broadband characterization of solid (polymer and glass) plates in a simple setup, where single spark events yielded high signal-to-noise ratio data without the need for critical alignment. This setup also enabled us to estimate pressure excursions approaching 10^5 Pa at millimeter-scale distances from the spark. The results are in large part made possible by the small size, wide bandwidth, and high sensitivity of the optomechanical sensor and might be of interest for air-coupled ultrasound applications in nondestructive testing.

There is a long-standing interest in air-coupled ultrasound (ACUS)[1] for nondestructive testing (NDT), since it eliminates the need for water immersion or gel-coupling and enables rapid-throughput inspection of diverse industrial materials.[2–10] ACUS setups must typically contend with extreme insertion losses (≫80 dB in some cases[1]) arising from air–solid impedance mismatches and the steep rise in air attenuation at MHz frequencies.[11]

The most established approach to ACUS uses narrowband (i.e., resonant) piezoelectric transducers, impedance-matched to air at a specific frequency.[1,2,8] Often the resonant frequencies of the transducer and sample must also be matched,[1] which limits the flexibility of the setup. Broadband capacitive transducers have been used to study a variety of solid samples.[4–7] However, both require sophisticated (i.e., high-voltage and -frequency) drive and receive electronics, and their relatively large size makes them directional at MHz frequencies, such that alignment is critical.[5] Optical microphones[3] are a promising alternative when combined with a broadband source of ultrasound, for example, generated using pulsed laser[3,9] or thermoacoustic[3,10] techniques.

Of related interest is the ultrasound produced by a low-energy spark discharge.[12–20] In its "near field,"[15] a spark produces a "blast wave" pulse,[17,20] which begins with a shock and a short compression phase followed by a longer rarefaction phase. At larger distances from the spark, the pulse can be approximated as an idealized "N-wave,"[13] with both an initial ("front") and final ("tail") shock. The front shock is characterized by a large (∼kPa) pressure increase on a timescale as short as ∼0.1 μs.[14–17] The pulse duration scales inversely with the discharge energy per unit length;[12] thus, lower-energy sparks produce higher-bandwidth acoustic signals, often extending into the MHz range. Experimental verification of such extreme pressure transients has been challenging, especially near the spark where the pressure excursions can greatly exceed the dynamic range of available instruments.[13] Moreover, capacitive microphones, and even optical interferometry methods,[14–16] are typically unable to fully resolve the front-shock rise time. Here, we report that low-cost piezoelectric spark igniters[21] produce high-amplitude shock pulses ($>10^4$ Pa near the spark) with wider bandwidth content than for previously reported spark sources.[13–19] Moreover, we show that an air-coupled optomechanical microphone has sufficient bandwidth to resolve these pulses and sufficient sensitivity to detect them in transmission through a variety of plastic and glass plates.

We used a recently reported[22] optomechanical microphone, which provides high sensitivity in air (noise-equivalent pressure, NEP ∼100 μPa/Hz$^{1/2}$) over a large bandwidth (several MHz). We have previously applied these devices to analysis and detection of low-pressure gas leaks[23] and to monitor the intrinsic thermal vibrations of small objects such as droplets[24] and bubbles.[25] Details on the particular sensor used here, including its calibration, are provided in the

supplementary material. We applied this sensor to the study of the acoustic pulses produced by several low-cost (~$10 USD) piezoelectric spark igniters. These units employ a button-actuated mechanical impact to generate ~20 kV across a piezoelectric cell, producing low-discharge-energy (<1 mJ)[21] sparks across millimeter-scale air gaps. Some of the results herein used a particular brand of simple camp-stove igniters ("Optimus Sparky"), which generates a spark between a central pin and an outer barrel (~3 mm spark gap, see Fig. 1). For through-plate measurements, we used a barbecue replacement part ("Master Chef OEM Piezo Igniter") designed to generate a spark between externally wired electrodes, which we label as "type B." This device produced slightly higher sound pressure levels (~1.5×, for similar gap lengths) but with more experimentally observed strike-to-strike variability, both possibly attributable to a noticeably stiffer spring mechanism. Additional details on the devices and the experimental setups are provided in the supplementary material.

Figure 1(a) shows a representative time-domain pressure signal received at ~12 cm distance from a single spark generated by a type A device. This is as close as we could place our microphone to the spark while keeping both the positive and negative pressure excursions within its linear dynamic range. As is typical,[13–16] the initial feature (highlighted by the dashed box) is a compression-rarefaction cycle intermediate between a blast-wave and an N-wave pulse.[13] The oscillations following this are attributable to acoustic reflections and diffraction within the microphone assembly.[13,15,20] The arrivals of reflected N pulses at delays of ~10, 20, and 40 μs corresponds to path delays of ~3–15 mm in air, close to the lateral dimensions of the microphone housing. Moreover, while the initial N-pulse was quite invariant with adjustments in the microphone angle (confirming the essentially omnidirectional characteristics of our sensors[22]), the remainder of the waveform was not. The trace shown was captured with the microphone at ~45° to the spark direction. These reverberations can be reduced by appropriate baffling.[13,14]

The half-wave duration ($T < 2.5$ μs) of these pulses is substantially shorter (by a factor of at least 3–4x) than those reported previously for spark-generated shock waves,[13–20] consistent with an inverse relationship between spark discharge energy and peak frequency of the generated ultrasound.[12] The piezo sparkers used have sub-millijoule discharge energies,[21] more than an order of magnitude lower than that for typical capacitor-based discharge setups.[13] Figure 1(b) shows the corresponding frequency-domain spectrum for the *N*-wave portion [indicated by the dashed box in part (a)]. Also shown is the energy spectrum predicted for an idealized *N*-wave given by[13]

$$|P(f)|^2 = 4P_s^2T^2\{j_1(2\pi fT)\}^2, \quad (1)$$

where P_s ~250 Pa is the peak pressure excursion, j_1 is the spherical Bessel function of the first kind and first order, and $T = 2.2$ μs was used in the fit. The peak frequency at ~150 kHz is considerably higher than previously reported for spark-generated ultrasound,[13–20] consistent with the short pulse length.

Given that the attenuation of ultrasound in air at 2 MHz is ~6.4 dB/cm,[11] it is remarkable that content in this range is observed beyond 10 cm. This is partly attributable to the nonlinear propagation of the transient acoustic shock,[13] which sharpens the pulse features and combats the low-pass filtering effect of air attenuation. Nevertheless, higher bandwidth and sharper features are expected nearer the spark. As shown in the supplementary material, the microphone could be biased to capture the front shock and initial compression phase at a distance as small as ~6 cm from the spark. This yielded a rise time estimate of ~0.16 μs, in good agreement with theoretically predicted values for similar sparks.[14,17] Content extending beyond 5 MHz is present in the corresponding frequency domain plot.

The spherical blast wave radiated by these low-energy sparks is expected to be within the limits of the so-called "weak shock theory."[13–15,17] It predicts that the peak pressure will exhibit power-law decay with distance; $P_{max}(r) \sim P_{max}(r_0)\cdot\exp(-\alpha\cdot r/r_0)$, where r_0 is a reference radial distance and α ~1.2–1.4 has typically been reported.[13,17,20] The yellow symbols in Fig. 2(a) indicate the peak positive excursion measured for distances in the 10–100 cm range. Each symbol is the average of multiple trials for a particular type A device, although the spark-to-spark variation was less than 5%, and similar pressure curves were measured for other devices (including type B devices with spark gap set to the same value of ~3 mm). The dashed curve is a power-law fit with $\alpha = 1.6$, representing slightly more rapid

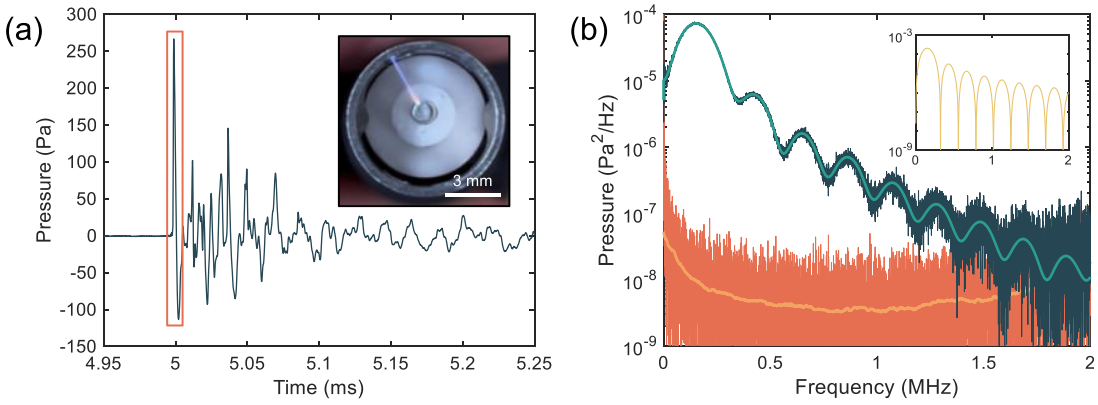

FIG. 1. (a) Typical time trace (at 12 cm spacing) of the pressure signal produced by a single spark event. The primary N-wave portion of the trace is indicated by the dashed box. The inset shows a typical spark produced by a type A device. (b) Non-averaged (single shot) energy spectrum of the primary N-wave pulse from part (a) (blue) alongside the noise-floor (dark orange). The overlaid curves show the zero-padded N-pulse spectrum (green) and the averaged noise floor (light orange). The inset shows the theoretical spectrum for an ideal N-pulse with same peak pressure and half-duration of 2.2 μs (yellow).

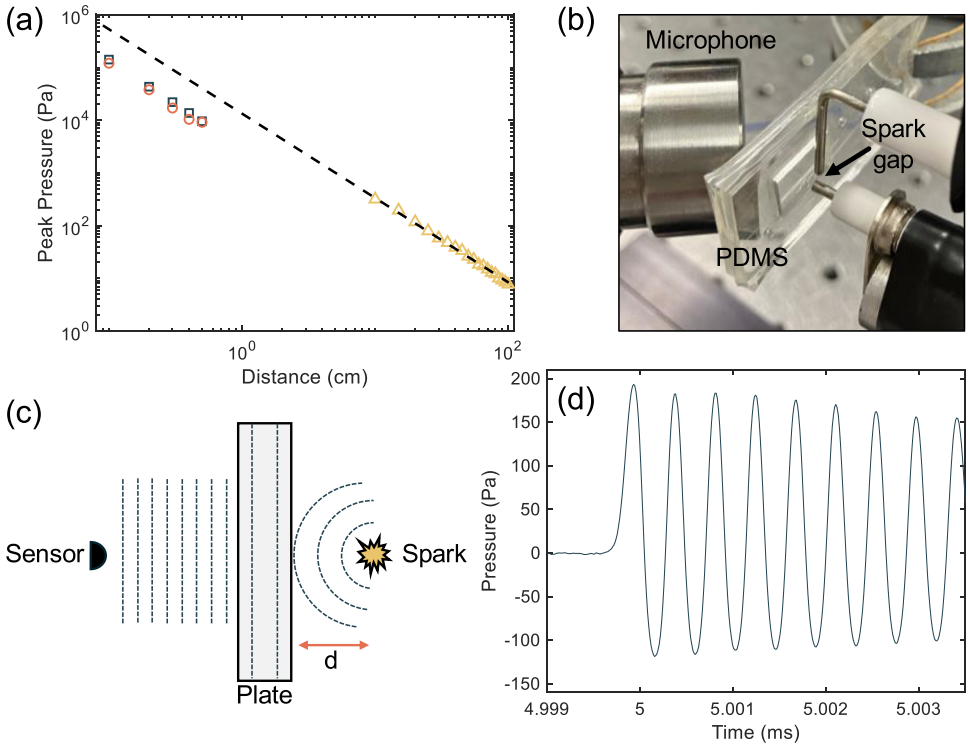

FIG. 2. (a) Peak positive pressure received at the microphone vs distance to the spark. At larger distances, the pressure was measured without an intervening PDMS layer (yellow triangles). The dashed line is a power-law fit to these data ($P_{max} \sim r^{-1.6}$). At shorter distances, the pressure was measured with either ∼4 mm (orange circles) or ∼2 mm (blue squares) of PDMS in the path, and the estimated peak pressure at the spark-side plate surface was plotted vs spacing between the spark gap and the PDMS (see main text). Each data point is an average of six measurements. (b) Photograph showing a PDMS sample (∼2 mm thick "window") between the spark gap and microphone. (c) Schematic illustration of the coupling of the spark blast-wave into a normal incidence compressional wave of an adjacent plate, a portion of which is transmitted to the small "point" sensor aligned opposite the spark. (d) A typical time trace of the initial pressure signal received on transmission through the ∼2 mm PDMS plate, showing a rise time on the order of 100 ns.

attenuation than for previously reported spark sources. We attribute this to the shorter pulse length and higher frequency content of these pulses, which increases the impact of air attenuation.[13,14]

As in the present case, dynamic range issues have typically limited electrical-microphone-based studies of spark pressure fields to distances greater than ∼10 cm.[13,14,17,18] However, Karzova *et al.*[16] used an optical schlieren method to estimate peak pressures as high as ∼12 kPa at 3 cm, and Liu *et al.*[15] used piezoelectric sensors to estimate a peak pressure as high as ∼60 kPa at 2.5 cm from a higher-energy spark. Here, we used a thin sheet of polydimethylsiloxane (PDMS) as an "acoustic attenuator" between the spark gap and the microphone, as shown in Figs. 2(b) and 2(c). Furthermore, we conservatively estimated the pressure produced by the spark as follows. First, we assume that the spherical blast wave acts as a purely normal force on the front surface of the plate and excites only a surface-normal longitudinal wave.[19] In reality, the divergent pressure field produced by the spark will also couple energy into off-normal shear and compressional waves.[1,8,26] Second, we assume that the optomechanical sensor predominately receives energy from the normal-incidence longitudinal wave. This is reasonable, since it is essentially a point sensor (∼100 μm in size) placed opposite the spark at a distance $>$ 5 mm from the plate. Moreover, even slightly off-normal wave components from the spark will tend to be totally reflected at the front plate surface,[1] and any energy that is coupled into off-normal plate modes will tend to "walk off" and be less efficiently radiated from the plate.

Based on these assumptions, we estimated the peak pressure at the front plate surface as the peak received pressure scaled by the normal-incidence reflection losses of the two air–PDMS interfaces. PDMS has an acoustic impedance of ∼1 MRayl (see the supplementary material for further details), which implies a loss of ∼28 dB at each air–PDMS interface. Thus, the first arrival of the blast-wave positive pressure excursion was assumed to be attenuated by 56 dB (i.e., due to the acoustic impedance mismatch between air and PDMS), corresponding to the pressure being reduced by a factor of ∼650. We carried out experiments with two different thicknesses of PDMS and varied the spark-PDMS spacing in the 1–5 mm range. A typical result is shown in Fig. 2(d), with a peak received pressure of nearly 200 Pa in spite of the intervening PDMS plate. These signals displayed a rapid initial increase in pressure, with a rise time of ∼0.1 μs, in good agreement with theory.[14] The oscillations following the initial pulse have a period of ∼0.4 μs and are due to excitation of the sensor fundamental resonance at ∼2.5 MHz. This indicates that significant energy is delivered through the plate, extending to several MHz (see Fig. 4). For a range of spacings, the peak received pressure was multiplied by 650 and plotted in Fig. 2(a) vs spark-PDMS distance. The results were relatively insensitive to PDMS thickness, supporting the earlier assumptions. This scaling is expected to underestimate the actual pressure, since it ignores all other sources of loss, including higher reflection at off-normal incidence, coupling to shear waves in the plate, as well as scattering and absorption.

It is interesting that these data points appear to follow the same power-law relationship, but with the estimated peak pressure lying at a factor of 4–5× lower than predicted by the fit to the large distance data points. Recalling that our data points essentially represent a lower limit (i.e., since some losses associated with the presence of the PDMS plate have been neglected), it is conceivable that the true pressure is nearer to the power-law predicted curve. In fact, Liu and Zhang[15] showed that weak shock theory was valid quite close to their higher

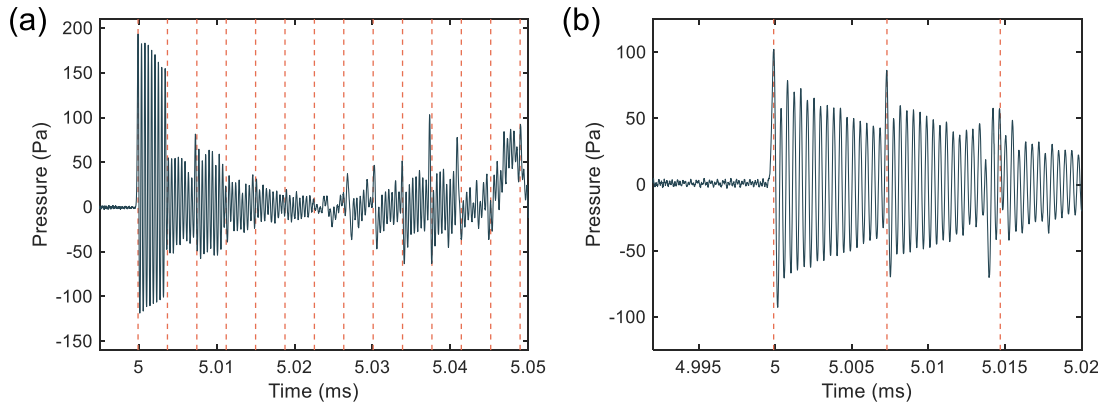

FIG. 3. (a) A typical waveform received on transmission through a 1.9 mm thick PDMS plate. The orange dashed lines indicate multiples of the expected round-trip transit time for the plate (b) as in part (a), except for a 3.8 mm thick PDMS plate.

energy sparks, where the pressure excursions were in a similar range to those estimated here. A more fulsome treatment of this experiment would require solution of nonlinear propagation equations[14] and consideration of the full set of plate modes,[1,8] but is left for future work.

The setup described in Figs. 2(b)–2(d) suggests a straightforward approach to ACUS characterization of plates. Notably, most previous setups used much larger sensors[3–8] and thus required critical alignment of the source, plate, and receiver in order to isolate the normal-incidence longitudinal waves and to avoid wavelength-scale averaging effects over the sensor surface.[5] Here, the small size of the optomechanical sensor ($<100\,\mu$m) implies that normal-incidence waves can be isolated simply by roughly aligning the sensor opposite the spark source. This was confirmed by studies of a variety of glass and plastic plates. For the results described herein, the spark-plate distance was set in the 1–2 mm range in order to maximize the signal-to-noise ratio (SNR). The spark gap was fixed at ∼2.5 mm, and the arc path was confirmed to lie between the electrodes and parallel to the plate surface (see the supplementary material). As an aside, we inspected the plates carefully under a microscope and observed no visible signs of damage, even after repeated spark discharges at a single location. All of the data shown was recorded for single-shot (i.e., single spark) pressure events, with no averaging.

Time traces for transmission through two different PDMS plates are shown in Fig. 3. As mentioned, the signal begins with a pressure shock and decaying oscillations at the ∼2.5 MHz frequency resonance of the sensor. However, the envelope of the signal is modulated by distinct phase and amplitude discontinuities. These discontinuities are periodically spaced, and the period is in good agreement with the round-trip delay times for a pulse circulating inside the PDMS. The dashed vertical lines indicate multiples of $t_{RT} = 2d/v$, where d is the plate thickness, and $v = 1030$ m/s is the longitudinal sound velocity for PDMS. Thus, the waveforms, rather complex for the thinner plate, can be interpreted as resulting from interference of multiple sub-reflected blast-wave pulses. The frequency-domain representations of these signals exhibit regularly spaced Fabry–Pérot fringes up to several MHz and are provided in the supplementary material.

We also studied plates with higher acoustic impedance. In these cases, it was typically more informative to view the data in the

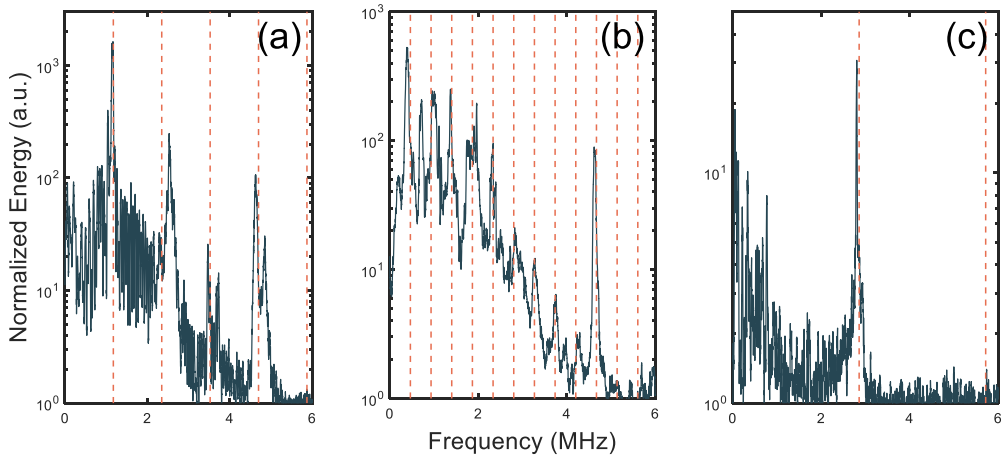

FIG. 4. Normalized energy spectra for (a) ∼1 mm thick polystyrene, (b) ∼3 mm thick acrylic, and (c) ∼1 mm thick borosilicate glass plates. The orange dashed lines indicate the predicted longitudinal Fabry–Pérot resonance frequencies in each case. See the main text and the supplementary material for additional details.

frequency domain.[4,7,8] Typical results are shown in Fig. 4, for a 1 mm thick polystyrene Petri dish, a 3 mm thick acrylic plate, and a 1 mm thick borosilicate glass slide (see the supplementary material for details). For each case, the fast Fourier transform (FFT) algorithm was applied to the received pulse, and the spectrum was normalized by dividing out the intrinsic background spectrum of our sensor.[23–25] Here, the orange dashed lines indicate the predicted longitudinal mode resonance frequencies ($f_m = m/t_{RT}$; $m = 1, 2, \ldots$). Additional details about the samples, including the sound velocities used, are provided in the supplementary material. Distinct resonant peaks are observed in each case, riding on a broad background of transmitted energy extending as high as ∼5 MHz for the plastic samples. Except for one or two extra peaks in Fig. 4(b), excellent alignment between the observed and predicted resonance frequencies is apparent in all cases. It is worth reiterating that these results were obtained without averaging or critical alignment but yielded an SNR similar or better than with conventional setups requiring both.[4,5,10] We hope to report more detailed and quantitative results in future work.

In summary, we have described an experimental study of the ultrasonic energy produced by low-cost, button-operated piezoelectric spark igniters. These units provide broadband and energetic ultrasound, with bandwidth extending up to at least 5 MHz and peak pressures on the order of 100 kPa near the spark.

In addition, we showed that an optomechanical microphone can be a unique enabler for ACUS setups, due to its high sensitivity, wide bandwidth, and small size. Coupled with the spark source, these properties facilitated a straightforward characterization of a variety of polymer and glass plates owing to the ease with which longitudinal plate resonances are isolated without critical alignment. This combination of a "point" source and receiver might present interesting options for NDT of solid materials.

See the supplementary material for additional information concerning the experimental setup, the optomechanical sensor, the commercial piezoelectric spark igniters, signal processing techniques, physical constants for the plate samples, and additional results.

The authors would like to acknowledge the following funding sources that supported this work: the Government of Alberta (Innovation Catalyst Grant), Mitacs (No. Accelerate IT38340), the Natural Sciences and Engineering Research Council of Canada (No. CREATE 495446-17), and the Alberta EDT Major Innovation Fund (Quantum Technologies).

AUTHOR DECLARATIONS

Conflict of Interest

Ultracoustics Technologies Ltd. (I, P) K.G.S., North Road Photonics Corp. (I, P) R.G.D.

Author Contributions

K. G. Scheuer: Conceptualization (equal); Data curation (equal); Funding acquisition (equal); Investigation (equal); Methodology (equal); Software (equal); Validation (equal); Visualization (equal); Writing – review & editing (equal). **R. G. DeCorby:** Conceptualization (equal); Data curation (equal); Formal analysis (equal); Funding acquisition (equal); Investigation (equal); Methodology (equal); Project administration (equal); Resources (equal); Validation (equal); Writing – original draft (equal); Writing – review & editing (equal).

DATA AVAILABILITY

The data that support the findings of this study are available from the corresponding author upon reasonable request.

REFERENCES

[1]E. Blomme, D. Bulcaen, and F. Declercq, "Air-coupled ultrasonic NDE: Experiments in the frequency range 750kHz–2MHz," NDT E Int. **35**(7), 417–426 (2002).
[2]D. E. Chimenti, "Review of air-coupled ultrasonic materials characterization," Ultrasonics **54**(7), 1804–1816 (2014).
[3]W. Essig, Y. Bernhardt, D. Döring, I. Solodov, T. Gautzsch, M. Gaal, D. Hufschläger, R. Sommerhuber, M. Brauns, T. Marhenke, J. Hasener, A. Szewieczek, and W. Hillger, "Air-coupled ultrasound—Emerging NDT method," ZfP-Zeitung **173**, 32–43 (2021).
[4]D. A. Hutchins, W. M. D. Wright, and D. W. Schindel, "Ultrasonic measurements in polymeric materials using air-coupled capacitance transducers," J. Acoust. Soc. Am. **96**(3), 1634–1642 (1994).
[5]D. W. Schindel and D. A. Hutchins, "Through-thickness characterization of solids by wideband air-coupled ultrasound," Ultrasonics **33**(1), 11–17 (1995).
[6]I. Ladabaum, X. Jin, H. T. Soh, A. Atalar, and B. T. Khuri-Yakub, "Surface micromachined capacitive ultrasonic transducers," IEEE Trans. Ultrason., Ferroelectr., Freq. Control **45**(3), 678–690 (1998).
[7]W. M. D. Wright and D. A. Hutchins, "Air-coupled ultrasonic testing of metals using broadband pulses in through-transmission," Ultrasonics **37**(1), 19–22 (1999).
[8]G. Waag, L. Hoff, and P. Norli, "Air-coupled ultrasonic through-transmission thickness measurements of steel plates," Ultrasonics **56**, 332–339 (2015).
[9]J. Rus and C. U. Grosse, "Thickness measurement via local ultrasonic resonance spectroscopy," Ultrasonics **109**, 106261 (2021).
[10]K. Bente, J. Rus, H. Mooshofer, M. Gaal, and C. U. Grosse, "Broadband air-coupled ultrasound emitter and receiver enable simultaneous measurement of thickness and speed of sound in solids," Sensors **23**(3), 1379 (2023).
[11]S. Takahashi, "Properties and characteristics of P(VDF/TrFE) transducers manufactured by a solution casting method for use in the MHz-range ultrasound in air," Ultrasonics **52**(3), 422–426 (2012).
[12]R. T. Harrold, in *IEEE International Conference on Electrical Insulation* (IEEE, 1980), pp. 184–189.
[13]W. M. Wright, "Propagation in air of N waves produced by sparks," J. Acoust. Soc. Am. **73**(6), 1948–1955 (1983).
[14]P. Yuldashev, S. Ollivier, M. Averiyanov, O. Sapozhnikov, V. Khokhlova, and P. Blanc-Benon, "Nonlinear propagation of spark-generated N-waves in air: Modeling and measurements using acoustical and optical methods," J. Acoust. Soc. Am. **128**(6), 3321–3333 (2010).
[15]Q. Liu and Y. Zhang, "Shock wave generated by high-energy electric spark discharge," J. Appl. Phys. **116**(15), 153302 (2014).
[16]M. M. Karzova, P. V. Yuldashev, V. A. Khokhlova, S. Ollivier, E. Salze, and P. Blanc-Benon, "Characterization of spark-generated N-waves in air using an optical schlieren method," J. Acoust. Soc. Am. **137**(6), 3244–3252 (2015).
[17]P. Yuldashev, M. Karzova, V. Khokhlova, S. Ollivier, and P. Blanc-Benon, "Mach-Zehnder interferometry method for acoustic shock wave measurements in air and broadband calibration of microphones," J. Acoust. Soc. Am. **137**(6), 3314–3324 (2015).
[18]X. Dai, J. Zhu, and M. R. Haberman, "A focused electric spark source for non-contact stress wave excitation in solids," J. Acoust. Soc. Am. **134**(6), EL513 (2013).

[19]J. A. Cooper, R. J. Dewhurst, S. Moody, and S. B. Palmer, "High-voltage spark discharge source as an ultrasonic generator," IEE Proc., Part A: Phys. Sci., Meas. Instrum., Manage. Educ. **131**(4), 275–281 (1984).
[20]C. Ayrault, P. Béquin, and S. Baudin, in *Acoustics 2012*, edited by S. F. d'Acoustique (Nantes, France, 2012).
[21]O. K. Jaenicke, F. G. Hita Martínez, J. Yang, S. Im, and D. B. Go, "Hand-generated piezoelectric mechanical-to-electrical energy conversion plasma," Appl. Phys. Lett. **117**(9), 093901 (2020).
[22]G. J. Hornig, K. G. Scheuer, E. B. Dew, R. Zemp, and R. G. DeCorby, "Ultrasound sensing at thermomechanical limits with optomechanical buckled-dome microcavities," Opt. Express **30**(18), 33083 (2022).
[23]K. G. Scheuer and R. G. DeCorby, "All-optical, air-coupled ultrasonic detection of low-pressure gas leaks and observation of jet tones in the MHz range," Sensors **23**(12), 5665 (2023).
[24]K. G. Scheuer, F. B. Romero, G. J. Hornig, and R. G. DeCorby, "Ultrasonic spectroscopy of sessile droplets coupled to optomechanical sensors," Lab Chip **23**, 5131–5138 (2023).
[25]K. G. Scheuer, F. B. Romero, and R. G. DeCorby, "Coupling the thermal acoustic modes of a bubble to an optomechanical sensor," arXiv:2308.01989.
[26]S. Dixon, C. Edwards, S. B. Palmer, and J. Reed, "Ultrasonic generation using a plasma igniter," J. Phys. D: Appl. Phys. **34**(7), 1075 (2001).